

## Prediction of slope stability using adaptive neuro-fuzzy inference system based on clustering methods

H. Fattahi

*Department of Mining Engineering, Arak University of Technology, Arak, Iran*

Received 24 April 2016; received in revised form 7 June 2016; accepted 8 June 2016  
Corresponding author: [h.fattahi@arakut.ac.ir](mailto:h.fattahi@arakut.ac.ir) (H. Fattahi).

### Abstract

Slope stability analysis is an enduring research topic in the engineering and academic sectors. Accurate prediction of the factor of safety (FOS) of slopes, their stability, and their performance is not an easy task. In this work, the adaptive neuro-fuzzy inference system (ANFIS) was utilized to build an estimation model for the prediction of FOS. Three ANFIS models were implemented including grid partitioning (GP), subtractive clustering method (SCM), and fuzzy c-means clustering method (FCM). Several important parameters such as cohesion coefficient, internal angle of friction, slope height, slope angle, and unit weight of slope material were utilized as the input parameters, while FOS was used as the output parameter. A comparison was made between these three models, and the results obtained showed the superiority of the ANFIS-SCM model. Also performance of the ANFIS-SCM model was compared with multiple linear regression (MLR). The results obtained demonstrated the effectiveness of the ANFIS-SCM model.

**Keywords:** *Slope Stability, Factor of Safety, ANFIS-Grid Partitioning, ANFIS-Subtractive Clustering Method, ANFIS-Fuzzy C-Means Clustering Method.*

### 1. Introduction

Slope stability has been considered as one of the most significant topics to study for the geotechnical society over many years [1]. Slope failures are natural phenomena that constitute a serious natural hazard in many countries. They are responsible for hundreds of millions of dollars of damage to the public and private property every year. To prevent or mitigate the landslide damage, slope stability analyses and stabilization require an understanding and evaluation of the processes that govern the behavior of the slopes. The factor of safety (FOS) based on an appropriate geotechnical model as a stability index is required in order to evaluate the slope stability. Many variables are involved in the slope stability evaluation, and calculation of FOS requires physical data on the geologic materials, geometrical data and its shear-strength parameters, information on pore-water pressures, etc. Traditionally, the methods available to solve FOS of a given slope are classified into the

categories including limit equilibrium method (LEM) [2-9], material point method (MPM) [1, 10], finite element method (FEM) [11-14], boundary element method (BEM) [15], finite element limit analysis [16], finite difference method (FDM) [17], numerical limit analysis methods [18], coupled Markov chain (CMC) model [19], slope stability probability classification (SSPC) method [20], strength reduction finite element method (SRFEM) [21], numerical back analysis [22], and finite element method-based shear strength reduction (FEM-SSR) [23].

Recently, soft computing approaches have been used successfully for modeling and classification. They are useful where the precise scientific tools are incapable of giving a low cost, analytic, and complete solution. The advantages of employing the soft computing approaches are their capability to tolerate imprecision, uncertainty, and partial truth to achieve tractability and robustness on

simulating human decision-making behavior with low cost.

Furthermore, in the recent years, in the field of the stability of slope modeling, with the development of cheaper personal computers, the intelligence system approaches have been increasingly used in the stability of slope analysis such as slope stability prediction using fuzzy logic (FL) [24-26], finding the critical FOS in slope stability analysis using simple genetic algorithm (GA) [27-29], using ant colony optimization algorithm [30], using particle swarm optimization (PSO) algorithm [31], and stability of slope prediction using artificial neural networks (ANNs). ANNs have some limitations, as follow:

- A major disadvantage of the ANN models is that, unlike other statistical models, they provide no information on the relative importance of the various parameters [32].
- In ANN, as the knowledge acquired during training is stored in an implicit manner, it is very difficult to come up with a reasonable interpretation of the overall structure of the network [33]. This lead to the term “black box”, which many researchers use while referring to the ANN behavior.
- In addition, ANN has some inherent drawbacks such as slow convergence speed, less generalizing performance, arriving at local minimum, and over-fitting problems.

In addition, the fuzzy set theory plays an important role in dealing with uncertainty when making decisions in engineering applications. Therefore, fuzzy sets have attracted a growing attention and interest in modern information technology, production technique, decision-making, pattern recognition, diagnostics, data analysis, etc.

Neuro-fuzzy systems are fuzzy systems, which use the ANN theory in order to determine their properties (fuzzy sets and fuzzy rules) by processing data samples. Neuro-fuzzy systems harness the power of the two paradigms FL and ANNs by utilizing the mathematical properties of ANNs in tuning rule-based fuzzy systems that approximate the way humans process information. A specific approach in the neuro-fuzzy development is the adaptive neuro-fuzzy inference system (ANFIS), which has shown significant results in modeling non-linear functions. In ANFIS, the membership function parameters are extracted from a data set that describes the system behavior. ANFIS learns features in the data set

and adjusts the system parameters according to a given error criterion.

In the following, the methodology of constructing the ANFIS model for prediction of FOS is presented. Three ANFIS models were implemented including grid partitioning (GP), subtractive clustering method (SCM), and fuzzy c-means clustering method (FCM). Several important parameters such as the cohesion coefficient, internal angle of friction, height of slope, slope angle, and unit weight of slope material were utilized as the input parameters, while FOS was the output parameter. The estimation abilities offered using the ANFIS models are presented using the field data in open source literatures.

## 2. Applied methods

### 2.1. Adaptive network-based fuzzy inference system

A fuzzy inference system can model the qualitative aspects of human knowledge and reasoning processes without employing precise quantitative analyses. Neural networks (NNs) are information-processing programs inspired by mammalian brain processes. NNs are composed of a number of inter-connected processing elements analogous to neurons. The training algorithm inputs to the NNs a set of input data, and checks the NN output desired result. Combining NNs with fuzzy logic (FL) has been shown to emulate the human process of expert decision-making reasonably. In traditional NNs, only weight values change during learning, and thus the learning ability of NNs is combined with the inference mechanism of FL for a neuro-fuzzy decision-making system [34].

An adaptive NN is a network structure consisting of several nodes connected through directional links. Each node is characterized by a node function with fixed or adjustable parameters. Once the fuzzy inference system (FIS) is initialized, the NN algorithms can be utilized to determine the unknown parameters (premise and consequent parameters of the rules) minimizing the error measure, as conventionally defined for each variable of the system. Due to this optimization procedure, the system is called adaptive [35].

The architecture of ANFIS consists of five layers, and a brief introduction of the model is as follows.

*Layer 1:* Each node  $i$  in this layer generates a membership grade of a linguistic label. For instance, the node function of the  $i^{th}$  node might be:

$$Q_i^1 = \mu_{A_i}(x) = \frac{1}{1 + \left[ \left( \frac{x - v_i}{\sigma_i} \right)^2 \right]^{b_i}} \quad (1)$$

where  $x$  is the input to node  $i$ , and  $A_i$  is the linguistic label (small, large, ...) associated with this node; and  $\{\sigma_i, v_i, b_i\}$  is the parameter set that changes the MF shapes. The parameters in this layer are referred to as the "premise parameters".

Layer 2: Each node in this layer calculates the "firing strength" of each rule via multiplication:

$$Q_i^2 = W_i = \mu_{A_i}(x) \cdot \mu_{B_i}(y) \quad i = 1, 2 \quad (2)$$

Layer 3: The  $i^{th}$  node of this layer calculates the ratio of the  $i^{th}$  rule's firing strength to the sum of all rules' firing strengths:

$$Q_i^3 = \bar{W}_i = \frac{w_i}{\sum_{j=1}^2 w_j}, \quad i = 1, 2 \quad (3)$$

For convenience, the outputs of this layer are called "normalized firing" strengths.

Layer 4: Every node  $i$  in this layer is a node function:

$$Q_i^4 = \bar{W}_i f_i = \bar{W}_i (p_i x + q_i y + r_i) \quad (4)$$

where  $\bar{W}_i$  is the output of layer 3. The parameters in this layer are referred to as "consequent parameters".

Layer 5: The single node in this layer is a circle node labeled R that computes the "overall output" as the summation of all incoming signals:

$$Q_i^5 = Overall\ Output = \sum \bar{W}_i f_i = \frac{\sum w_i f_i}{\sum w_i} \quad (5)$$

For a given data set, different ANFIS models can be constructed using different identification methods. GP, SCM, and FCM are three methods utilized in this study to identify the antecedent MFs.

### 2.1.1. Grid partitioning of antecedent variables

This approach proposes independent partitions of each antecedent variable [35]. The expert developing the model can define the MFs of all antecedent variables using prior knowledge and experience. They are designed to represent the meaning of the linguistic terms in a given context. However, for many systems, no specific

knowledge is available on these partitions. In that case, the domains of the antecedent variables can simply be partitioned into a number of equally spaced and equally-shaped MFs. Thus in the GP approach, the domain of each antecedent variable is partitioned into equidistant and identically shaped MFs. Using the available input-output data, the MF parameters can be optimized.

### 2.1.2. Subtractive clustering method

SCM was introduced by Chiu [36], and its data points are considered as the candidates for center of clusters. The algorithm continues as follows:

At first, a collection of  $n$  data points  $\{X_1, X_2, X_3, \dots, X_n\}$  in an  $M$ -dimensional space is considered. Since each data point is a candidate for cluster center, a density measure at data point  $X_i$  is defined as:

$$D_i = \sum_{j=1}^n \exp \left( - \frac{\|x_i - x_j\|^2}{\left( \frac{r_a}{2} \right)^2} \right) \quad (6)$$

where  $r_a$  is a positive constant. Therefore, a data point will have a high density value if it has many neighboring data points. The radius  $r_a$  defines a neighborhood; data points outside this radius contribute only slightly to the density measure. After the density measure of each data point has been calculated, the data point with the highest density measure is selected as the first cluster center. Let  $X_{c1}$  be the point selected, and  $D_{c1}$  be its density measure. Next, the density measure for each data point  $x_i$  is revised as follows:

$$D_i = D_i - D_{c1} \exp \left( - \frac{\|x_i - x_{c1}\|^2}{\left( \frac{r_b}{2} \right)^2} \right) \quad (7)$$

where  $r_b$  is a positive constant. After the density calculation for each data point is revised, the next cluster center  $X_{c2}$  is selected, and all of the density calculations for data points are revised again. This process is repeated until a sufficient number of cluster centers is generated.

SCM is an attractive approach to the synthesis of ANFIS networks, which estimates the cluster number and its location automatically. In the subtractive clustering algorithm, each sample

point is seen as a potential cluster center. Using this approach, the computation time becomes linearly proportional to the data size but independent from the dimension problem under consideration [37, 38]. Using SCM, the cluster center of all data was found out. Then the numbers of subtractive centers were utilized to generate automatic MFs and rule base as well as the location of MF within dimensions. This method is a fast clustering method (unlike GP and FCM), designed for high-dimension problems with a moderate number of data points. This is because its computation grows linearly with the data dimension and as the square of the number of data points.

**2.1.3. Fuzzy c-means clustering method**

FCM is a data clustering algorithm introduced by Bezdek [39], in which each data point belongs to a cluster to a degree specified by a membership grade. FCM partitions a collection of  $n$  vectors,  $X_i, i = 1, 2, \dots, n$ , into  $C$  fuzzy groups, and finds a cluster center in each group such that a cost function of dissimilarity measure is minimized. The stages of the FCM algorithm are, therefore, first described in brief. At first, the cluster centers  $c_i, i = 1, 2, \dots, C$  randomly from the  $n$  points  $\{X_1, X_2, X_3, \dots, X_n\}$  are chosen. Then the membership matrix  $U$  is computed using the following equation:

$$\mu_{ij} = \frac{1}{\sum_{k=1}^c \left(\frac{d_{ij}}{d_{kj}}\right)^{\frac{2}{m-1}}} \tag{8}$$

where  $d_{ij} = \|c_i - x_j\|$  is the Euclidean distance between the  $i^{th}$  cluster center and the  $j^{th}$  data point, and  $m$  is the fuzziness index. Then the cost function is computed according to the following equation. The process is stopped if it is below a certain threshold.

$$J(U, c_1, \dots, c_2) = \sum_{i=1}^c J_i = \sum_{i=1}^c \sum_{j=1}^n \mu_{ij}^m d_{ij}^2 \tag{9}$$

In the final step, the new  $c$  fuzzy cluster centers  $c_i, i = 1, 2, \dots, C$  are computed using the following equation:

$$c_i = \frac{\sum_{j=1}^n \mu_{ij}^m x_j}{\sum_{j=1}^n \mu_{ij}^m} \tag{10}$$

**2.2. Multiple linear regression**

Multiple linear regression (MLR) is an extension of the regression analysis that incorporates additional independent variables in the predictive equation. Here, the model to be fitted is:

$$y = C_1 + C_2x_2 + \dots + C_nx_n + e \tag{11}$$

where  $y$  is the dependent variable,  $x$  is the independent random variable, and  $e$  is a random error that is the amount of variation in  $y$  not accounted for by the linear relationship. Parameter  $C$ , standing for the regression coefficients, is unknown and is to be estimated. However, there is usually a substantial variation in the observed points around the fitted regression line. The deviation of a particular point from the regression line (its predicted value) is called the residual value. The smaller the variability of the residual values around the regression line, the better is the model prediction.

**3. Inputs and output data**

The main scope of this work was to implement the above methodology in the problem of slope stability prediction. In order to forecast FOS in the case of soil slopes, the factors that influence FOS have to be determined. The dataset applied in this study for determining the relationship among the set of input and output variables was gathered from open sources literature [40-44]. The input layer data consists of six input parameters in the case of circular failure. The parameters that were selected were related to the geotechnical properties and the geometry of each slope. More specifically, the parameters used for circular failure were unit weight ( $\gamma$ ), cohesion ( $C$ ), slope angle ( $\beta$ ), height ( $H$ ), angle of internal friction ( $\varphi$ ), and pore pressure ratio ( $r_u$ ). The output layer composed of a single output parameter (FOS).

The data set consisted of 67 case studies of the slopes analyzed for the circular critical failure mechanism. The original data covering the 67 case studies are presented in Table 1. Also the descriptive statistics of all the data sets are shown in Table 2.

**Table 1. Training and testing data sets used for constructing models (Sah et al. [40]\*, Hoek and Bray [41]\*\*, Hudson [42]\*\*\*, Lin et al. [43]\*\*\*\*, and Madzic [44]\*\*\*\*\*).**

Case No.	Input parameters						FOS	Location
	$\gamma$ (KN/m <sup>3</sup> )	C (KPa)	$\rho(^{\circ})$	$\beta(^{\circ})$	H (m)	$r_u$		
1	18.68	26.34	15	35	8.23	0	1.11	Congress street, open cut slope, Chicago, USA
2	16.5	11.49	0	30	3.66	0	1	Brightlingsea slide UK
3	18.84	14.36	25	20	30.5	0	1.875	Unknown
4	18.84	57.46	20	20	30.5	0	2.045	Unknown
5	28.44	29.42	35	35	100	0	1.78	Case 1: open-pit iron ore mine, India
6	28.44	39.23	38	35	100	0	1.99	Case 2: open-pit iron ore mine, India
7	20.6	16.28	26.5	30	40	0	1.25	Open-pit chromite mine, Orissa, India
8	14.8	0	17	20	50	0	1.13	Sarukuygi landslide, Japan
9	14	11.97	26	30	88	0	1.02	Case 1: open-pit iron ore mine, Goa, India
10	25	120	45	53	120	0	1.3	Mercoirol open-pit coal mine, France
11	26	150.05	45	50	200	0	1.2	Marquesade open-pit iron ore mine, Spain
12	18.5	25	0	30	6	0	1.09	Unknown
13	18.5	12	0	30	6	0	0.78	Unknown
14	22.4	10	35	30	10	0	2	Case 1: Highvale coal mine, Alberta, Canada
15	21.4	10	30.34	30	20	0	1.7	Case 2: Highvale coal mine, Alberta, Canada
16	22	20	36	45	50	0	1.02	Case 1: open-pit coal mine, Newcastle coalfield, Australia
17	22	0	36	45	50	0	0.89	Case 2: open-pit coal mine, Newcastle coalfield, Australia
18	12	0	30	35	4	0	1.46	Unknown
19	12	0	30	45	8	0	0.8	Unknown
20	12	0	30	45	4	0	1.44	Unknown
21	12	0	30	45	8	0	0.86	Unknown
22	23.47	0	32	37	214	0	1.08	Pima open-pit mine, Arizona, USA
23	16	70	20	40	115	0	1.11	Case 1: Wyoming, USA
24	20.41	33.52	11	16	10.67	0.35	1.4	Seven Sisters Landslide, UK
25	19.63	11.97	20	22	12.19	0.405	1.35	Case 1: The Northolt slide, UK
26	21.82	8.62	32	28	12.8	0.49	1.03	Selset Landslide, Yorkshire, UK
27	20.41	33.52	11	16	45.72	0.2	1.28	Saskatchewan dam, Canada
28	18.84	15.32	30	25	10.67	0.38	1.63	Case 2: The Northolt slide, UK
29	18.84	0	20	20	7.62	0.45	1.05	Sudbury slide, UK
30	21.43	0	20	20	61	0.5	1.03	Folkstone Warren slide, Kent, UK
31	19.06	11.71	28	35	21	0.11	1.09	River bank side, Alberta, Canada
32	18.84	14.36	25	20	30.5	0.45	1.11	Unknown
33	21.51	6.94	30	31	76.81	0.38	1.01	Unknown
34	14	11.97	26	30	88	0.45	0.625	Case 2: open-pit iron ore mine, Goa, India
35	18	24	30.15	45	20	0.12	1.12	Athens slope, Greece
36	23	0	20	20	100	0.3	1.2	Open-pit coal mine Allori coalfield, Italy
37	22.4	100	45	45	15	0.25	1.8	Case 1: open-pit coal mine, Alberta, Canada

**Table 1. Continued.**

38	22.4	10	35	45	10	0.4	0.9	Case 2: open-pit coal mine, Alberta, Canada
39	20	20	36	45	50	0.25	0.96	Case 3: open-pit coal mine, Newcastle coalfield, Australia
40	20	20	36	45	50	0.5	0.83	Case 4: open-pit coal mine, Newcastle coalfield, Australia
41	20	0	36	45	50	0.25	0.79	Case 5: open-pit coal mine, Newcastle coalfield, Australia
42	20	0	36	45	50	0.5	0.67	Case 6: open-pit coal mine, Newcastle coalfield, Australia
43	22	0	40	33	8	0.35	1.45	Case 1: Harbour slope, Newcastle, Australia
44	24	0	40	33	8	0.3	1.58	Case 2: Harbour slope, Newcastle, Australia
45	20	0	24.5	20	8	0.35	1.37	Case 3: Harbour slope, Newcastle, Australia
46	18	5	30	20	8	0.3	2.05	Case 4: Harbour slope, Newcastle, Australia
47	21	20	40	40	12	0	1.84	Unknown
48	21	45	25	49	12	0.3	1.53	Unknown
49	21	30	35	40	12	0.4	1.49	Unknown
50	21	35	28	40	12	0.5	1.43	Unknown
51	20	10	29	34	6	0.3	1.34	Unknown
52	20	40	30	30	15	0.3	1.84	Unknown
53	18	45	25	25	14	0.3	2.09	Unknown
54	19	30	35	35	11	0.2	2	Unknown
55	20	40	40	40	10	0.2	2.31	Unknown
56	18.85	24.8	21.3	29.2	37	0.5	1.07	Unknown
57	18.85	10.34	21.3	34	37	0.3	1.29	Unknown
58	18.8	30	10	25	50	0.1	1.4	Unknown
59	18.8	25	10	25	50	0.2	1.18	Unknown
60	18.8	20	10	25	50	0.3	0.97	Unknown
61	19.1	10	10	25	50	0.4	0.65	Unknown
62	18.8	30	20	30	50	0.1	1.46	Unknown
63	18.8	25	20	30	50	0.2	1.21	Unknown
64	18.8	20	20	30	50	0.3	1	Unknown
65	19.1	10	20	30	50	0.4	0.65	Unknown
66	22	20	22	20	180	0	1.12	Unknown
67	22	20	22	20	180	0.1	0.99	Unknown

\* Cases 1–46. \*\* Cases 47–55. \*\*\* Cases 56–57. \*\*\*\* Cases 58–65. \*\*\*\*\* Cases 66–67.

**Table 2. Statistical description of dataset utilized for construction of models.**

Parameter	Min.	Max.	Average
Unit weight ( $\gamma$ )	12.00	28.44	19.71
Cohesion (C)	0.00	150.05	22.25
Angle of internal friction ( $\varphi$ )	0.00	45.00	26.23
Slope angle ( $\beta$ )	16.00	53.00	32.47
Height (H)	3.66	214.00	44.15
Pore pressure ratio ( $r_u$ )	0.00	0.50	0.20
Factor of safety (FOS)	0.63	2.31	1.29

#### 4. Pre-processing of data and performance criteria

In the data-driven system modeling methods, some pre-processing steps are commonly implemented prior to any calculation to eliminate any outliers, missing values or bad data. This step ensures that the raw data retrieved from the

database is perfectly suitable for modeling. In order to soften the training procedure and improve the accuracy of prediction, all data samples are normalized to adapt to the interval [0, 1]

according to the following linear mapping function:

$$x_M = \frac{x - x_{\min}}{x_{\max} - x_{\min}} \quad (12)$$

Where  $x$  is the original value from the dataset,  $x_M$  is the mapped value, and  $x_{\min}$  ( $x_{\max}$ ) denotes the minimum (maximum) raw input values, respectively. It is to be noted that the model outputs were remapped to their corresponding real values by the inverse mapping function ahead of calculating any performance criterion. Furthermore, to evaluate the performances of the ANFIS and MLR models, root-mean-squared-error (RMSE), mean squared error (MSE), and squared correlation coefficient ( $R^2$ ) were chosen to be the measure of accuracy.  $N$  is the number of samples, and  $y$  and  $y'$  are the measured and predicted values, respectively. RMSE, MSE, and  $R^2$  could be defined, respectively, as follow:

$$RMSE = \sqrt{\frac{1}{N} \sum_{i=1}^N (y_i - y'_i)^2} \quad (13)$$

$$MSE = \frac{1}{N} \sum_{i=1}^N (y_i - y'_i)^2 \quad (14)$$

$$R^2 = 1 - \frac{\sum_{i=1}^N (y_i - y'_i)^2}{\sum_{i=1}^N y_i^2 - \frac{(\sum_{i=1}^N y_i)^2}{N}} \quad (15)$$

### 5. Prediction of factor of safety using ANFIS models

In this work, ANFIS was utilized to build a prediction model for the assessment of FOS from the available data using the MATLAB environment. Three ANFIS models were implemented, including grid partitioning (GP), subtractive clustering method (SCM), and fuzzy c-means clustering method (FCM). Figure 1 shows the fuzzy architecture of ANFIS. A dataset that includes 67 data points was employed in the current study, while 53 data points (80%) were utilized for constructing the model, and the remaining data points (14 data points) were utilized for assessment of the degree of accuracy and robustness.

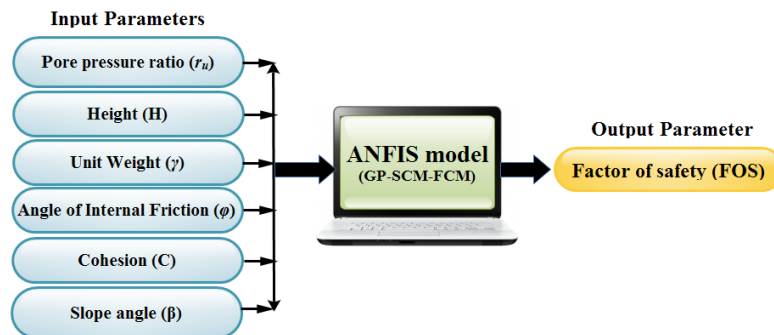


Figure 1. Architecture of ANFIS based on GP, SCM, and FCM.

The training and testing procedures of the three ANFIS models (GP, SCM, and FCM) were conducted from scratch for the five mentioned datasets. The RMSE, MSE, and  $R^2$  values obtained for training datasets indicate the capability of learning the structure of data samples, whereas the results of testing dataset reveal the generalization potential and the

robustness of the system modeling methods. The characterizations of the ANFIS models were tabulated in Table 3.

The number of rules obtained for the GP, SCM, and FCM models were 729, 37, and 25, respectively. MFs of the input parameters for different models are shown in Figures 2-4.

Table 3. Characterizations of ANFIS models.

ANFIS parameter	ANFIS-GP	ANFIS-SCM	ANFIS-FCM
MF type	Gaussian	Gaussian	Gaussian
Output MF	Linear	Linear	Linear
Number of nodes	1503	527	359
Number of linear parameters	5103	259	175
Number of nonlinear parameters	36	444	300
Total number of parameters	5139	703	475
Number of training data pairs	53	53	53
Number of testing data pairs	14	14	14
Number of fuzzy rules	729	37	25

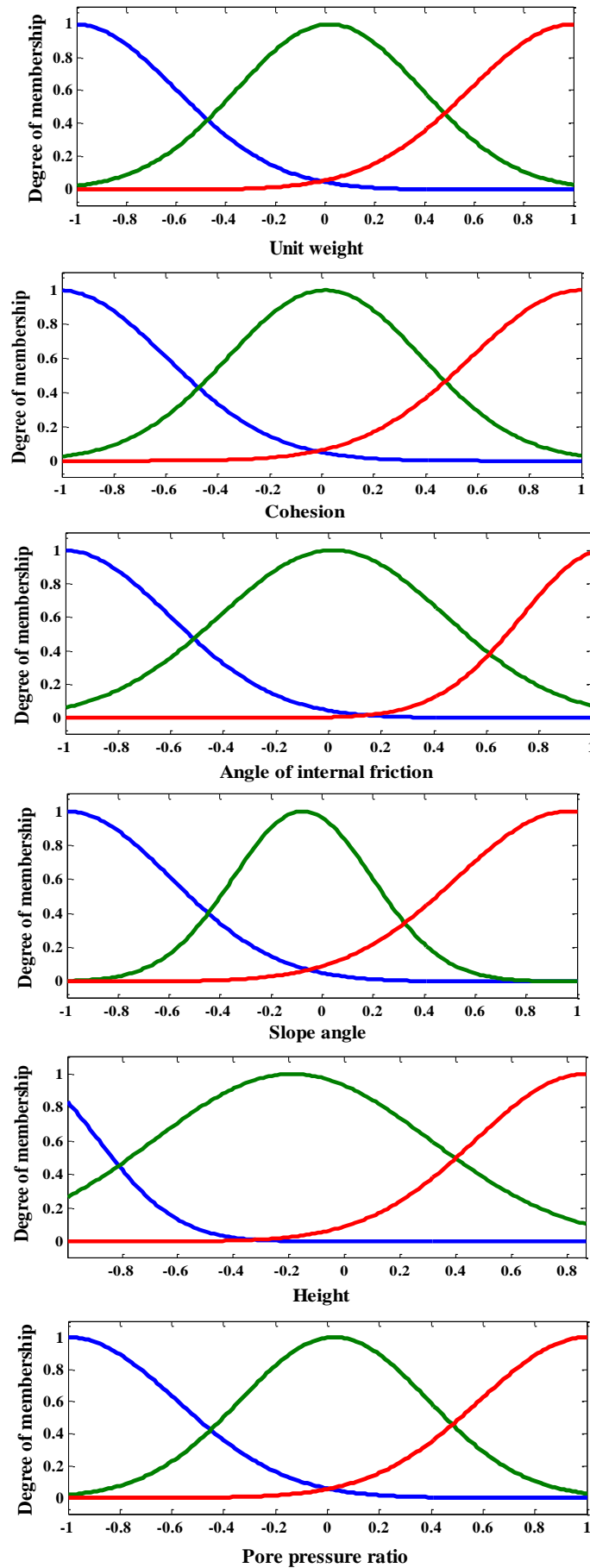


Figure 2. MFs obtained by ANFIS-GP model.

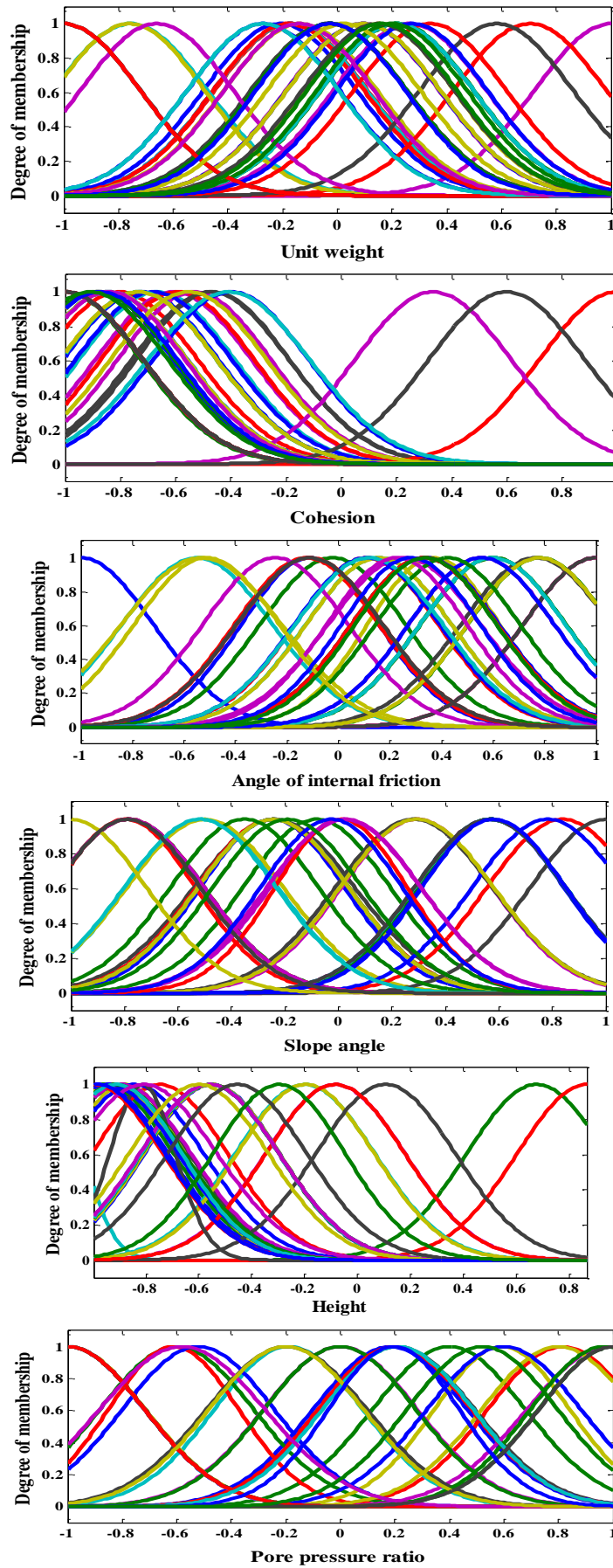


Figure 3. MFs obtained by ANFIS-SCM model.

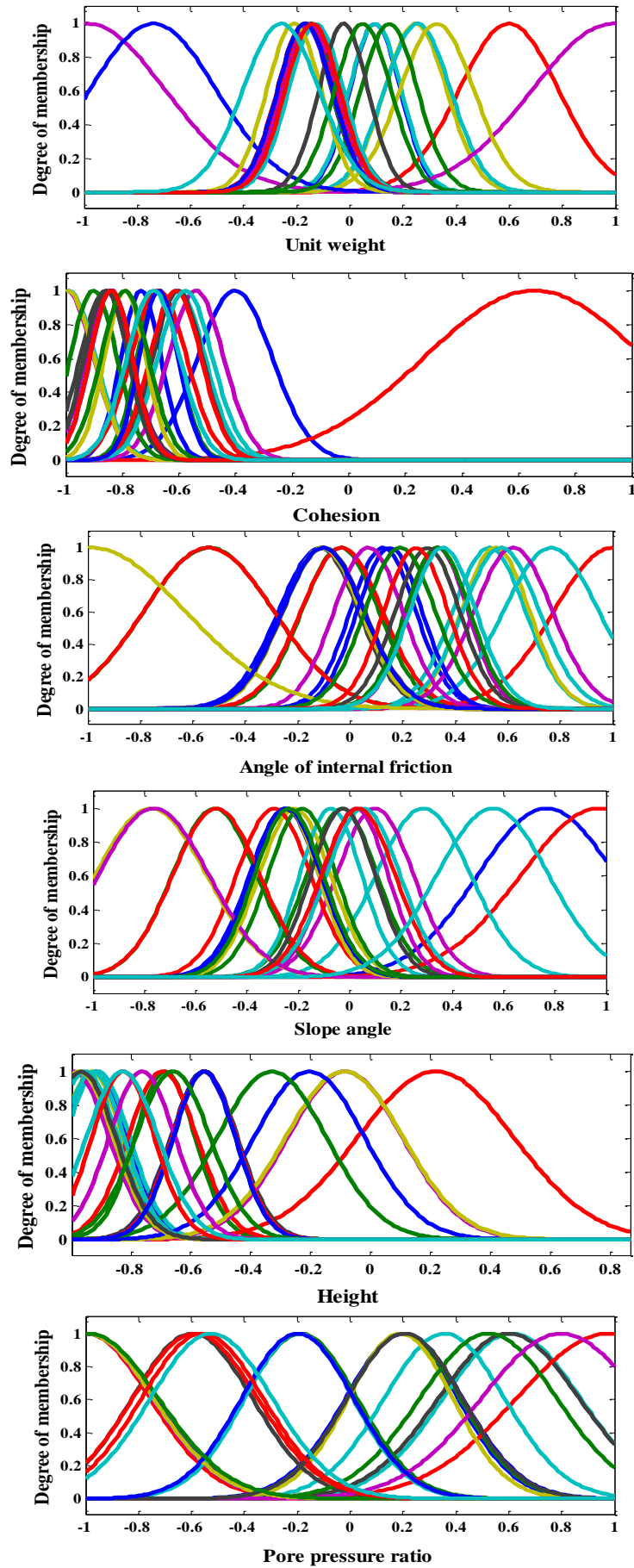


Figure 4. MFs obtained by ANFIS-FCM model.

A comparison between the results of the three models for testing datasets is shown in Table 4. As it can be observed in this table, the ANFIS-SCM model with RMSE=0.205, MSE=0.042 and  $R^2=0.852$  for the testing datasets performs better than the other two models for prediction of FOS. Also the performance analysis of the three models for training datasets is shown in Table 5. The performance indices obtained in Tables 4 and 5 indicate the high performance of the ANFIS-SCM model that can be utilized successfully for the prediction of FOS. Furthermore, correlations between the measured and predicted values of FOS for testing and training phases are shown in Figures 5-7. Also a comparison between the predicted FOS values by the ANFIS models and the measured values for the ANFIS models for testing and

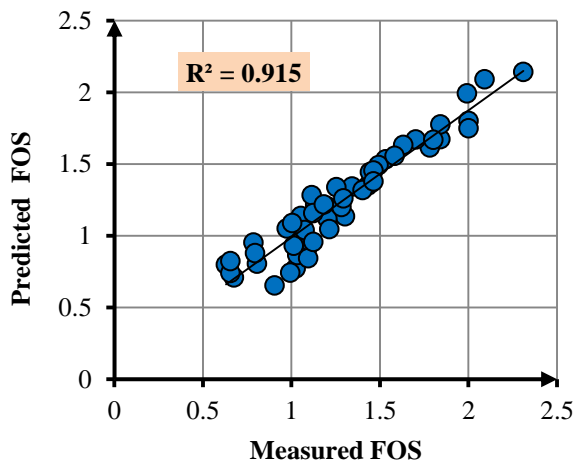
training datasets is shown in Figures 8 and 9, respectively. As shown in these figures, the results of the ANFIS-SCM model, in comparison with the actual data, show a good precision of the ANFIS-SCM model.

**Table 4. A comparisons between results of three models for testing datasets.**

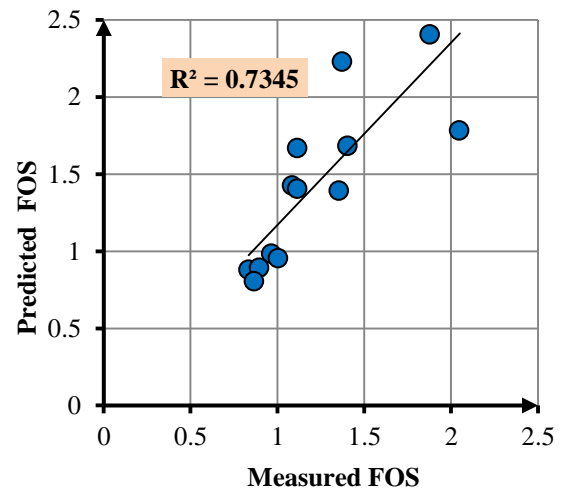
ANFIS model	RMSE	MSE	$R^2$
ANFIS-GP	0.446	0.199	0.735
ANFIS-SCM	0.205	0.042	0.852
ANFIS-FCM	0.360	0.129	0.658

**Table 5. A comparisons between results of three models for training datasets.**

ANFIS model	RMSE	MSE	$R^2$
ANFIS-GP	0.149	0.022	0.915
ANFIS-SCM	0.109	0.012	0.952
ANFIS-FCM	0.155	0.024	0.939

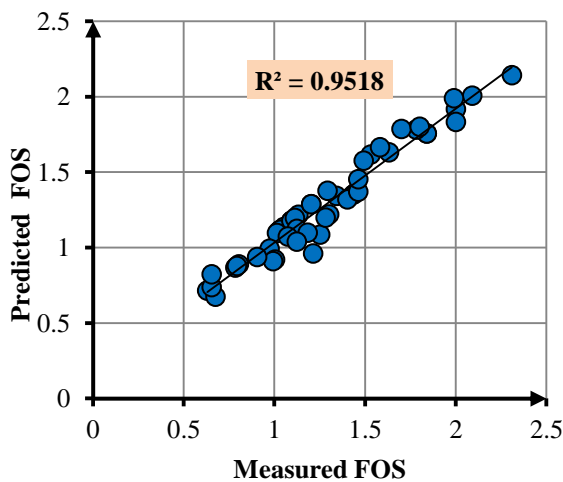


(a)

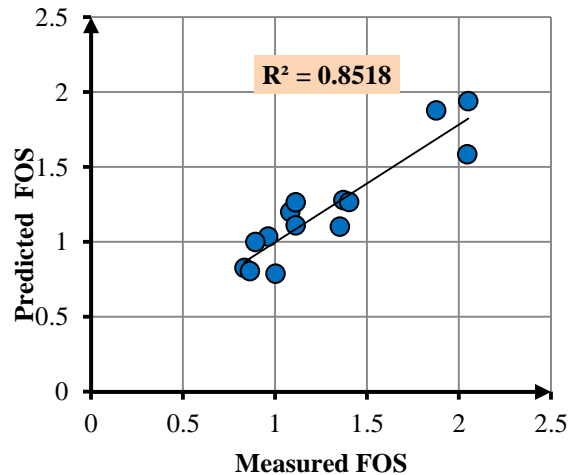


(b)

**Figure 5. Correlation between measured and predicted FOS values by ANFIS-GP model: a) training data, and b) testing data.**



(a)



(b)

**Figure 6. Correlation between measured and predicted FOS values by ANFIS-SCM model: a) training data, and b) testing data.**

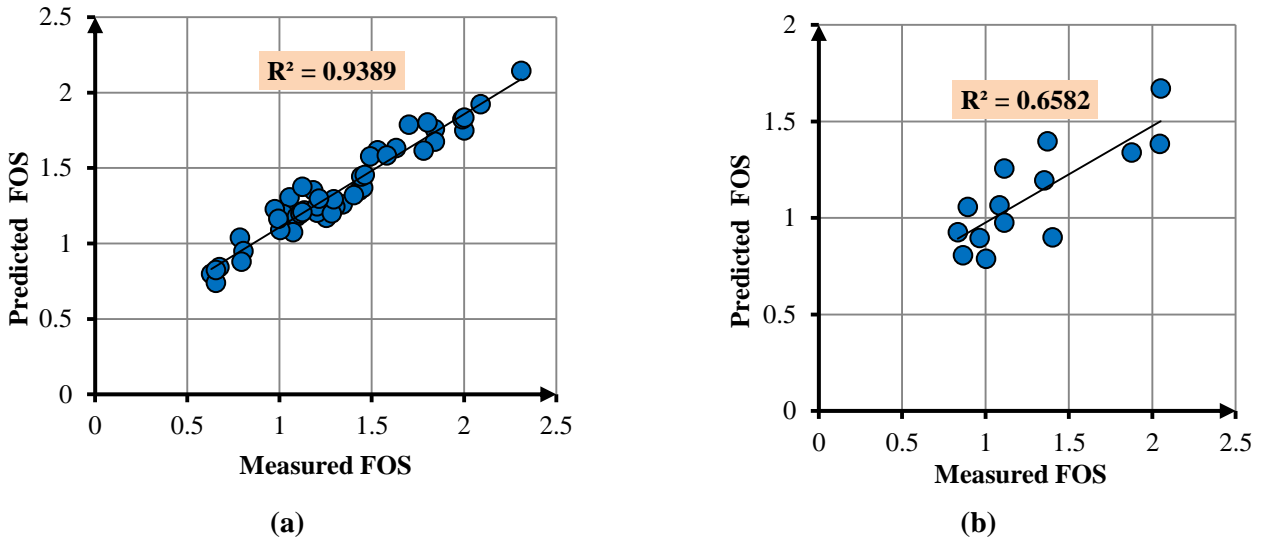


Figure 7. Correlation between measured and predicted FOS values by ANFIS-FCM model: a) training data, and b) testing data.

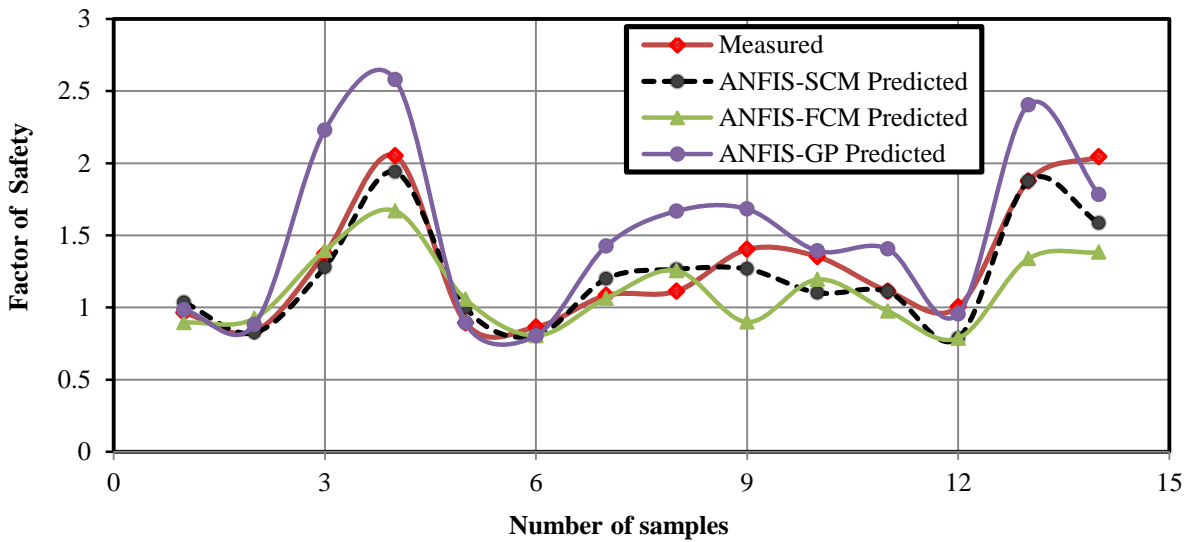


Figure 8. Comparison between measured and predicted FOS by ANFIS models for testing datasets.

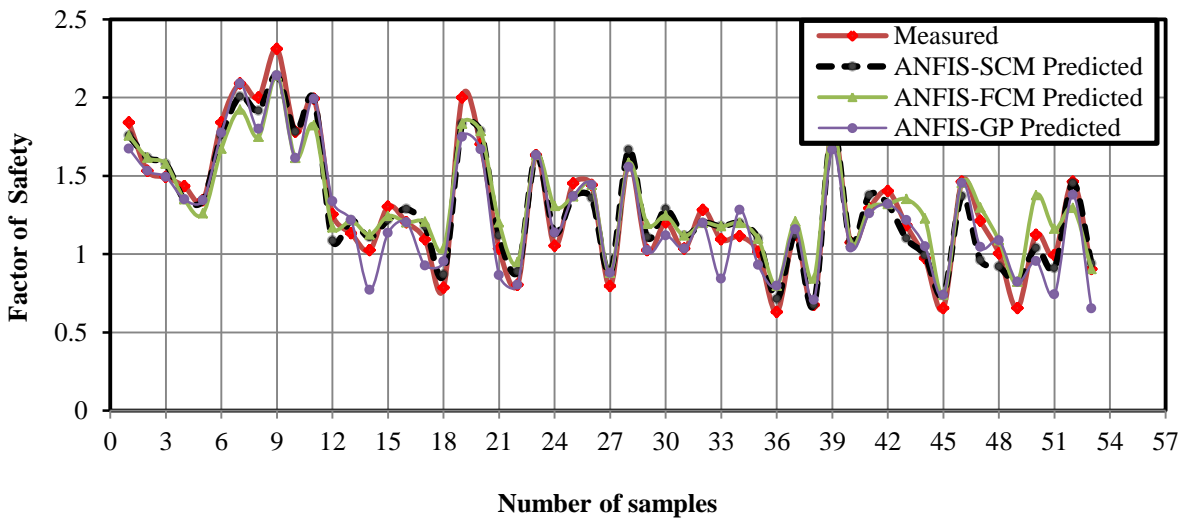


Figure 9. Comparison between measured and predicted FOS by ANFIS models for training datasets.

**6. Prediction of factor of safety using multiple linear regression**

In this work, a regression analysis was performed using the training and test data employed in the ANFIS model. FOS was considered as the dependent variable, and unit weight ( $\gamma$ ), cohesion (C), slope angle ( $\beta$ ), height (H), angle of internal friction ( $\phi$ ), and pore pressure ratio ( $r_u$ ) were considered as the independent variables. A computer-based package called SPSS (Statistical Package for the Social Sciences) was used to carry out the regression analysis. The estimated regression relationships for FOS are given as follow:

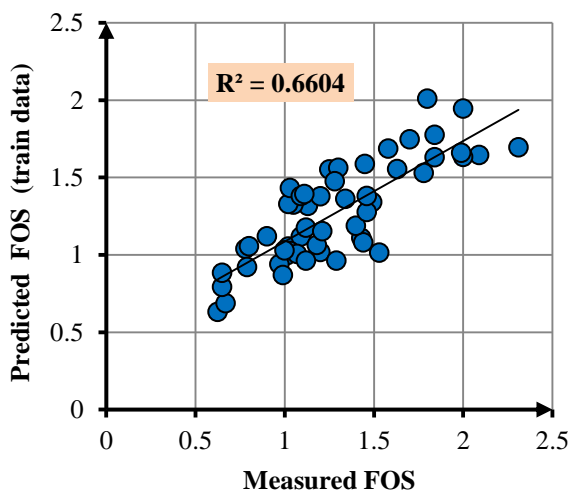
$$FOS = 1.422 + 0.026\gamma + 0.006C + 0.024\phi - 0.03\beta - 0.006H - 0.939r_u \quad (16)$$

The statistical results of the model are given in Table 6. The FOS was estimated according to Eq. (16). Figure 10 shows the correlation between the measured FOS and those predicted using MLR with six inputs.

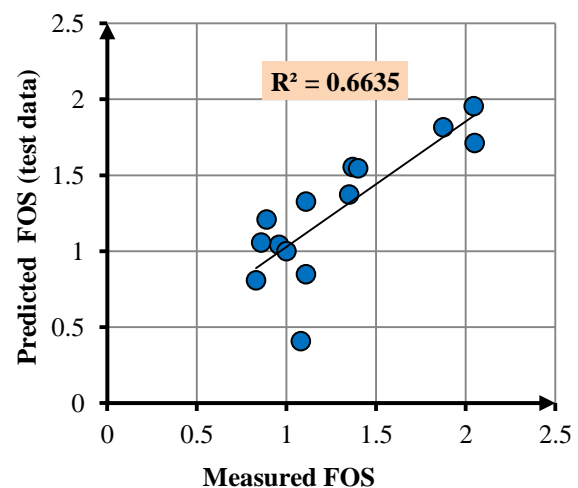
Table 7 compares R<sup>2</sup>, MSE, and RMSE associated with the two methods for both the training and test data. In both states of using the training and testing data, the performance indices obtained in Table 7 indicate the high performance of the ANFIS-SCM model that can be used successfully for the prediction of FOS. Low correlation values between the model predictions and measured data using the MLR method describes its low capability in the prediction of FOS.

**Table 6. Statistical characteristics of multiple regression models.**

Model	Method	Independent variables	Coefficient	Standard error	Standard error of estimate	t value	F ratio	Sig. level	Determination coefficient (R <sup>2</sup> )
Eq. 16	Enter	Constant	1.422	0.273	0.249	5.203	14.969	0.000	0.661
		$\gamma$	0.026	0.013		2.060		0.045	
		C	0.006	0.002		4.023		0.000	
		$\phi$	0.024	0.005		5.123		0.000	
		$\beta$	-0.030	0.006		-5.173		0.000	
		H	-0.006	0.001		-6.616		0.000	
		$r_u$	-0.939	0.206		-4.554		0.000	



(a)



(b)

**Figure 10. Comparison of predicted MLR and measured FOS: a) training data, and b) testing data.**

**Table 7. Comparison of results (R<sup>2</sup>, MSE, RMSE) of two methods in training and testing data.**

Method	R <sup>2</sup> (train data)	R <sup>2</sup> (test data)	MSE (train data)	MSE (test data)	RMSE (train data)	RMSE (test data)
ANFIS-SCM	0.952	0.852	0.012	0.042	0.109	0.205
MLR	0.660	0.664	0.054	0.084	0.233	0.289

## 7. Conclusions

The prediction of FOS for the circular slope failure assessment using the three ANFIS models (GP, SCM, and FCM) suggests that this might prove to be a useful alternative, with distinct advantages over the LEMs. The advantage of the ANFIS model in the analysis of slope stability problems over the traditional LEMs is that no assumption is required to be made in advance about the shape or location of the failure surface, slice side forces, and their directions. Furthermore, the following remarks can be concluded:

- A comparison was made between the three ANFIS models GP, SCM, and FCM using 67 data samples, and based upon the performance indices; RMSE, MSE and  $R^2$ , ANFIS-SCM with RMSE=0.205, MSE=0.042 and  $R^2=0.852$  was selected as the best predictive model.
- In comparison between the ANFIS-SCM and MLR models, the low correlation values between the model predictions and the measured data using the MLR method describes its low capability in the prediction of FOS.
- Consequently, it can be concluded that ANFIS-SCM is a reliable system modeling technique for predicting FOS with highly acceptable degrees of accuracy and robustness.
- This study shows that the ANFIS approach can be applied as a powerful tool for modeling some problems involved in rock mechanics engineering.

## References

[1]. Bhandari, T., Hamad, F., Moormann, C., Sharma, KG. and Westrich, B. (2016). Numerical modelling of seismic slope failure using MPM. *Comput Geotech.* 75: 126-134. doi:<http://dx.doi.org/10.1016/j.compgeo.2016.01.017>.

[2]. Cheng, Y., Lansivaara, T. and Wei, W. (2007). Two-dimensional slope stability analysis by limit equilibrium and strength reduction methods. *Comput Geotech.* 34 (3):137-150.

[3]. Yu, H., Salgado, R., Sloan, S. and Kim, J. (1998). Limit analysis versus limit equilibrium for slope stability. *J Geotech Geoenviron.* 124 (1): 1-11.

[4]. Zhang, J-F. and Ding, H. (2005). Generalized 3D limit-equilibrium method for slope stability analysis and its application. *Chin J Rock Mech Eng.* 3 (1).

[5]. Nash, D. (1987). Comparative Review of Limit Equilibrium Methods of Stability Analysis. *Slope*

*Stability: Geotechnical Engineering and Geomorphology* John Wiley and Sons New York 1987 p 11-75. 43 fig. 6 tab. 70 ref.

[6]. Zhu, D., Lee, C. and Jiang, H. (2003). Generalised framework of limit equilibrium methods for slope stability analysis. *Geotechnique.* 53 (4):377-395.

[7]. Nash, D. (1981). A comparative review of limit equilibrium methods of stability analysis. *Slope Stability.* MG Anderson. & KS Richards. Eds: 11-75.

[8]. Qi, C., Wu, J., Liu, J. and Kanungo, D.P. (2016). Assessment of complex rock slope stability at Xiari. southwestern China. *Bull Eng Geology Envir.* 75 (2): 537-550. doi:10.1007/s10064-015-0763-4.

[9]. Gu, T., Wang, J., Fu, X. and Liu, Y. (2015). GIS and limit equilibrium in the assessment of regional slope stability and mapping of landslide susceptibility. *Bull Eng Geology Envir.* 74 (4): 1105-1115. doi:10.1007/s10064-014-0689-2.

[10]. Wang, B., Vardon, P.J. and Hicks, M.A. (2016). Investigation of retrogressive and progressive slope failure mechanisms using the material point method. *Comput Geotech* 78: 88-98. doi:<http://dx.doi.org/10.1016/j.compgeo.2016.04.016>.

[11]. Griffiths, D. and Lane, P. (1999). Slope stability analysis by finite elements. *Geotechnique.* 49 (3): 387-403.

[12]. Duncan, J.M. (1996). State of the art: limit equilibrium and finite-element analysis of slopes. *J Geotech Eng.* 122 (7): 577-596.

[13]. Griffiths, D. and Fenton, G.A. (2004). Probabilistic slope stability analysis by finite elements. *J Geotech Geoenviron* 130 (5): 507-518.

[14]. Luo, N., Bathurst, R.J. and Javankhoshdel, S. (2016). Probabilistic stability analysis of simple reinforced slopes by finite element method. *Comput Geotech.* 77: 45-55.

[15]. Martel, S.J. and Muller, J.R. (2000). A two-dimensional boundary element method for calculating elastic gravitational stresses in slopes. *Pure Appl Geophys.* 157 (6-8): 989-1007.

[16]. Tschuchnigg, F., Schweiger, H.F. and Sloan, S.W. (2015). Slope stability analysis by means of finite element limit analysis and finite element strength reduction techniques. Part II: Back analyses of a case history. *Comput Geotech.* 70: 178-189. doi:<http://dx.doi.org/10.1016/j.compgeo.2015.07.019>.

[17]. Sun, S., Sun, H., Wang, Y., Wei, J., Liu, J. and Kanungo, D.P. (2014). Effect of the combination characteristics of rock structural plane on the stability of a rock-mass slope. *Bull Eng Geology Envir.* 73 (4): 987-995. doi:10.1007/s10064-014-0593-9.

[18]. Lim, K., Li, A.J. and Lyamin, A.V. (2015). Three-dimensional slope stability assessment of two-

layered undrained clay. *Comput Geotech.* 70: 1-17. doi:http://dx.doi.org/10.1016/j.compgeo.2015.07.011.

[19]. Li, D-Q., Qi, X-H., Cao, Z-J., Tang, X-S., Phoon, K-K. and Zhou, C-B. (2016). Evaluating slope stability uncertainty using coupled Markov chain. *Comput Geotech.* 73: 72-82. doi:http://dx.doi.org/10.1016/j.compgeo.2015.11.021.

[20]. Li, X.Z. and Xu, Q. (2016). Application of the SSPC method in the stability assessment of highway rock slopes in the Yunnan province of China. *Bull Eng Geology Envir.* 75 (2): 551-562. doi:10.1007/s10064-015-0792-z.

[21]. Jiang, Q., Qi, Z., Wei, W. and Zhou, C. (2015). Stability assessment of a high rock slope by strength reduction finite element method. *Bull Eng Geology Envir.* 74 (4):1153-1162. doi:10.1007/s10064-014-0698-1.

[22]. Salmi, E.F. and Hosseinzadeh, S. (2015). Slope stability assessment using both empirical and numerical methods: a case study. *Bull Eng Geology Envir.* 74 (1): 13-25. doi:10.1007/s10064-013-0565-5.

[23]. Kaya, A. (2016). Geotechnical assessment of a slope stability problem in the Citlakkale residential area (Giresun, NE Turkey). *Bull Eng Geology Envir.* pp. 1-15. doi:10.1007/s10064-016-0896-0.

[24]. Pradhan, B. (2010). Application of an advanced fuzzy logic model for landslide susceptibility analysis. *Inte J Comput Intell Syst.* 3 (3): 370-381.

[25]. Saboya Jr F., da Glória Alves M., Dias Pinto W (2006). Assessment of failure susceptibility of soil slopes using fuzzy logic. *Eng Geol* 86 (4):211-224.

[26]. Ercanoglu, M. and Gokceoglu, C. (2002). Assessment of landslide susceptibility for a landslide-prone area (north of Yenice, NW Turkey) by fuzzy approach. *Environ Geol.* 41 (6): 720-730.

[27]. McCombie, P. and Wilkinson, P. (2002). The use of the simple genetic algorithm in finding the critical factor of safety in slope stability analysis. *Comput Geotech.* 29 (8): 699-714.

[28]. Zolfaghari, A.R., Heath, A.C. and McCombie, P.F. (2005). Simple genetic algorithm search for critical non-circular failure surface in slope stability analysis. *Comput Geotech.* 32 (3): 139-152.

[29]. Tun, Y.W., Pedroso, D.M., Scheuermann, A. and Williams, D.J. (2016). Probabilistic reliability analysis of multiple slopes with genetic algorithms. *Comput Geotech.* 77: 68-76. doi:http://dx.doi.org/10.1016/j.compgeo.2016.04.006.

[30]. Kahatadeniya, K.S., Nanakorn, P. and Neaupane, K.M. (2009). Determination of the critical failure surface for slope stability analysis using ant colony optimization. *Eng Geol.* 108 (1): 133-141.

[31]. Cheng, Y., Li, L., Chi, S-c. and Wei, W. (2007). Particle swarm optimization algorithm for the location

of the critical non-circular failure surface in two-dimensional slope stability analysis. *Comput Geotech.* 34 (2): 92-103.

[32]. Park, D. and Rilett, L.R. (1999). Forecasting freeway link travel times with a multilayer feedforward neural network. *Computer-Aided Civil and Infrastructure Engineering.* 14 (5): 357-367.

[33]. Kecman, V. (2001). Learning and soft computing: support vector machines. neural networks. and fuzzy logic models. MIT press.

[34]. Lin, C.T. and Lee, C.S.G. (1991). Neural-network-based fuzzy logic control and decision system. *IEEE T Comput* 40 (12): 1320-1336.

[35]. Jang, J.S.R. (1993). ANFIS: Adaptive-network-based fuzzy inference system. *IEEE T Syst Man Cyb* 23 (3): 665-685.

[36]. Chiu, S.L. (1994). Fuzzy model identification based on cluster estimation. *J Intell Fuzzy Syst.* 2 (3): 267-278.

[37]. Smuda, J., Dold, B., Friese, K., Morgenstern, P. and Glaesser, W. (2007). Mineralogical and geochemical study of element mobility at the sulfide-rich Excelsior waste rock dump from the polymetallic Zn-Pb-(Ag-Bi-Cu) deposit. Cerro de Pasco, Peru. *J Geochem Explor.* 92 (2): 97-110.

[38]. Stavroulakis, P. (2004). Neuro-fuzzy and Fuzzy-neural Applications in Telecommunications (Signals and Communication Technology). Springer.

[39]. Bezdek, J.C. (1973). Fuzzy mathematics in pattern classification. Cornell university. Ithaca.

[40]. Sah, N., Sheorey, P. and Upadhyaya, L. (1994). Maximum likelihood estimation of slope stability. *Int J Rock Mech Min Sci.* 31 (1): 47-53.

[41]. Bray, J.W. and Hoek, E. (1981). Rock slope engineering. Taylor & Francis.

[42]. Hudson, J. (1992). Rock engineering systems. Theory and practice. Ellis Horwood Limited. West Sussex.

[43]. Lin, P., Su, M., Lin, M. and Lee, T. (1998). Investigation on the failure of a building constructed on a hillslope: Proc 2nd International Symposium on Field Measurements in Geomechanics. Kobe. 6-9 April 1987 V1. P547-555. Publ Rotterdam: AA Balkema. 1988. In: International Journal of Rock Mechanics and Mining Sciences & Geomechanics Abstracts. 1990. vol 2. Pergamon. p A114.

[44]. Madzic, E. (1988). Stability of unstable final slope in deep open iron mine. Landslides Balkema. Rotterdam. 1: 455-458.

## پیش‌بینی پایداری شیروانی با استفاده از سیستم استنتاج عصبی- فازی تطبیقی بر مبنای روش‌های کلاسترینگ

هادی فتاحی

دانشکده مهندسی معدن، دانشگاه صنعتی اراک، اراک، ایران

ارسال ۲۰۱۶/۴/۲۴، پذیرش ۲۰۱۶/۶/۱۸

\* نویسنده مسئول مکاتبات: h.fattahi@arakut.ac.ir

### چکیده:

امروزه یکی از مباحث مهندسی و مراکز علمی دانشگاهی تجزیه و تحلیل در زمینه پایداری شیروانی است. پیش‌بینی دقیق ضریب ایمنی شیروانی‌ها و تحلیل پایداری آن‌ها کار ساده‌ای نیست. به همین منظور در این تحقیق از سیستم استنتاج عصبی- فازی تطبیقی (انفیس) برای پیش‌بینی ضریب ایمنی شیروانی‌ها استفاده شده است. سه مدل انفیس شامل انفیس- پارتیشن‌بندی شبکه، انفیس- کلاسترینگ تفریقی و انفیس- کلاسترینگ C-means فازی برای مدل‌سازی به کار گرفته شده است. در این مدل‌ها ورودی‌ها شامل: چسبندگی، زاویه اصطکاک داخلی، ارتفاع شیروانی، زاویه شیروانی و وزن مخصوص ماده تشکیل‌دهنده شیروانی می‌باشند در حالی که ضریب ایمنی به عنوان خروجی مدل‌ها در نظر گرفته شده است. در مقایسه بین مدل‌ها، نتایج نشان از برتری مدل انفیس- کلاسترینگ تفریقی می‌دهد. همچنین در این تحقیق عملکرد انفیس- کلاسترینگ تفریقی با رگرسیون خطی چند متغیره مقایسه شده است که نتایج همچنان نشان از برتری عملکرد انفیس- کلاسترینگ تفریقی می‌دهد.

**کلمات کلیدی:** پایداری شیروانی، ضریب ایمنی، انفیس- پارتیشن‌بندی شبکه، روش انفیس- کلاسترینگ تفریقی، روش انفیس- کلاسترینگ C-means فازی.